The Simultaneous Inference of Stratospheric NO_2–H_2O and HNO_3–CF_2Cl_2 Using Limb Sounding Radiometry

JAMES M. RUSSELL III

NASA Langley Research Center, Hampton, VA 23665

LARRY L. GORDLEY

Systems and Applied Sciences Corporation, Hampton, VA 23665

(Manuscript received 31 October 1978, in final form 12 June 1979)

ABSTRACT

An inversion algorithm has been developed to simultaneously infer the concentrations of two gases with overlapping spectral signatures using limb emission measurements. The algorithm is efficient and provides a solution in two or three iterations. It has been tested in a simulation study for the inference of stratospheric NO_2–H_2O and HNO_3–CF_2Cl_2. Existing satellite instrumentation was the basis for errors used in the calculations. These included noise, scale and bias errors, angular registration errors, spacecraft motion effects, and effects due to a finite instrument field of view. It is estimated that concentrations of all four gases can be measured globally from a satellite with errors of less than 20%.

1. Introduction

The stratosphere is a stable region of our atmosphere that exhibits little vertical mixing. Anthropogenic activity has created potential threats to the integrity of this region through injections of chemicals which can cause catalytic ozone destruction (e.g., NO_x, ClO_x, BrO_x). This input is of particular concern because the upper atmosphere tends to retain these gases for long time periods allowing the destructive reactions to gradually deplete ozone. Our state of knowledge concerning these effects is growing, but a global data base is needed in order to better understand the physical processes occurring especially with regard to the interactions between radiation, dynamics and chemistry. As a result, numerous measurements of important chemical constituents have been made from airborne platforms, and satellite measurements are planned using limb sounding by both thermal emission and solar occultation methods. The Nimbus 7 satellite, launched 24 October, 1978, promises to provide a significant global data base on ozone and important gases in the NO_x chemistry from the Limb Infrared Monitor of the Stratosphere (LIMS) experiment, the Stratosphere and Mesosphere Sounder (SAMS), and the Solar Backscatter Ultraviolet/Total Ozone Monitor System (SBUV/TOMS). Both LIMS and SAMS are thermal limb sounding experiments. The LIMS measures radiance profiles which are processed to yield the vertical distributions of temperature, O_3, NO_2, HNO_3 and H_2O, while SAMS provides measurements of temperature, CO, CH_4, N_2O, NO and H_2O. The SBUV/TOMS measures O_3 profiles above the peak and total ozone in a vertical column. Also, the Halogen Occultation Experiment (HALOE) is under development to provide satellite solar occultation measurements of compounds involved in the ClO_x, NO_x, and HO_x chemistry (Russell *et al.*, 1977).

The standard procedure in the thermal emission experiment is to first infer the temperature profile from measurements in the emission band of a gas with known atmospheric mixing ratio (e.g., 15 μm CO_2 band), and then to use these data along with measurements in an emission band of another gas whose mixing ratio is to be inferred. This approach works well if a spectral region can be isolated that contains only emission due to the gas of interest. This is rarely the case with limb emission, however, since broad spectral filters are needed in order to maximize the energy collected. Usually several gases emit in a given region. With judicious choice of filter location, the effect of these unwanted emissions can be minimized most of the time so that only second-order corrections are required. These corrections can be made mostly with estimates or crude measurements of the concentrations of the gases causing the contaminant signal. There are some notable exceptions such as NO_2–H_2O spectral overlap at 6.0 μm, CH_4–H_2O overlap at 7.8 μm, and HNO_3–CF_2Cl_2 at 11.0 μm. As an

0022-4928/79/112259-08$06.00

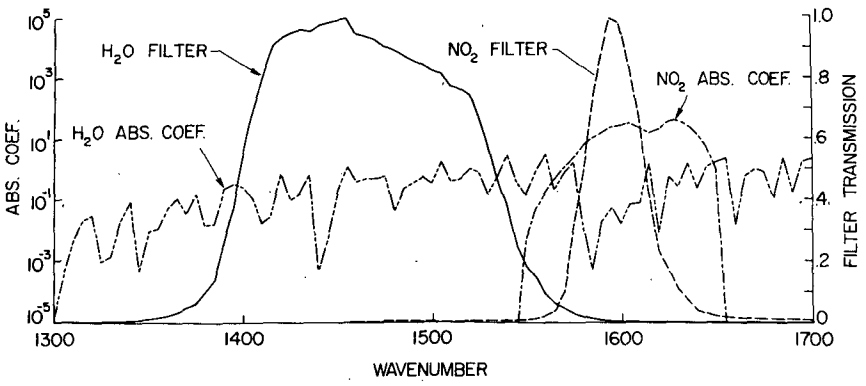

FIG. 1. NO_2–H_2O absorption coefficients (atm^{-1} cm^{-1} at P = 1 atm, T = 250 K) and filter functions.

example of this, Fig. 1 shows absorption coefficients and typical spectral filter positions for measurement of NO_2 and H_2O in the 6.0 μm region. Depending on the final location of spectral filters, there may be significant interdependence of signals from such channels, suggesting the need for a simultaneous inversion scheme. There are other instrument approaches, such as the pressure modulated radiometer (PMR), that may alleviate the spectral overlap problem due to the inherent high spectral resolution of the technique. Application of the PMR, however, brings with it a set of instrument problems different than those for the broad-band radiometer, and it is not the intent of this paper to discuss the relative merits of these techniques. The purpose of this paper is to describe an iterative algorithm for use in the broad-band limb experiment to infer concentrations of two gases with spectrally overlapping emission. The algorithm is applied in a simulated inversion study to show its usefulness and to determine expected errors in global measurements of NO_2, H_2O, HNO_3 and CF_2Cl_2 using instrumentation having performance characteristics typical of existing instrumentation.

2. The inversion algorithm

The limb emission $N(\Delta\nu)$ for a ray with tangent height H_0 (Fig. 2) can be expressed by

$$N(\Delta\nu) = \int_{\Delta\theta}\int_{\Delta\tau}\int_{\Delta\nu} B(\nu,T) \times d\tau(\nu,q,P,T)\gamma(\theta)\phi(\nu)d\nu d\theta, \quad (1)$$

where B is the Planck function at wavenumber ν and temperature T, τ the transmittance from the spacecraft to any point along the ray path across the horizon extending to cold space, q mixing ratio, P pressure, $\phi(\nu)$ the spectral filter function with bandwidth $\Delta\nu$, and $\gamma(\theta)$ the instrument spatial field of view function. In this paper, we are assuming that two radiance measurements are made in spectral regions defined by filter $\phi_1(\nu)$ and $\phi_2(\nu)$. These data are to be used for inferring the mixing ratios of constituents 1 and 2.

It is assumed that the temperature solution can be obtained by a method like that of Gille and House (1971). We start the development of a relaxation equation for constituent inversion by adopting the "instant inversion" scheme of House and Ohring (1969). The basis of this technique is the fact that for limb viewing, most of the radiance is emitted from a narrow layer just above the tangent height. As an example, the weighting function or change in transmittance along the horizontal ray path with respect to altitude is shown in Fig. 3 for the 9.6 μm ozone band at selected tangent heights. Note the sharpness of the weighting functions for alti-

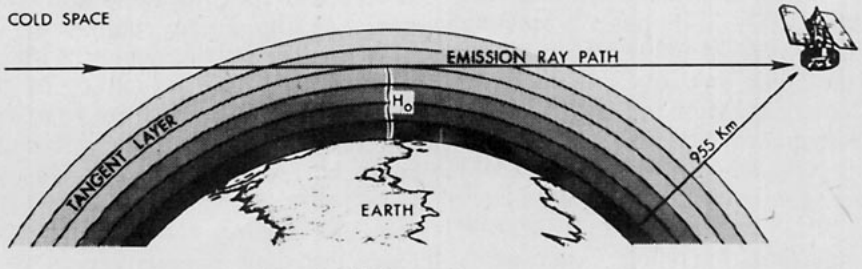

FIG. 2. Limb experiment geometry.

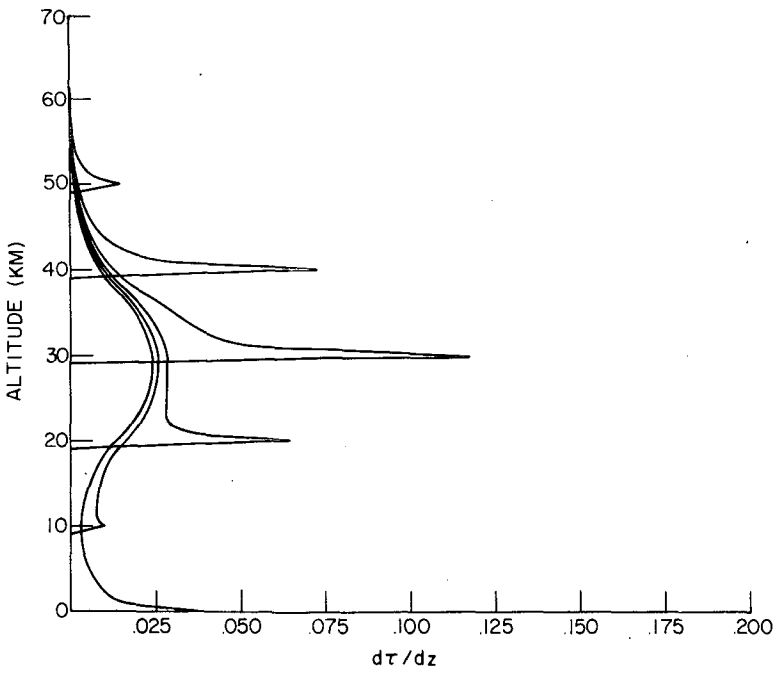

FIG. 3. Limb experiment ozone weighting functions for the 9.6 μm band at selected tangent heights.

tudes $\gtrsim$20 km. The "instant inversion" approach makes use of this feature to approximate Eq. (1) by the expression

$$N(\nu) \approx B[\nu_1, T(H_0')][1 - \tau(\nu, P_e)], \qquad (2)$$

where monochromatic radiation and an infinitesimal spatial field of view are assumed. The quantity H_0' is the altitude corresponding to the centroid of the weighting function for a given tangent height. The horizon path is treated as a single layer having a transmittance $\tau(\nu, P_e)$ from the spacecraft across the horizon to cold space. The transmittance for constituent i can be expressed as

$$\tau_i(\nu, P_e) = \exp[-K_i q_i P_e l_e], \qquad (3)$$

where K_i is the absorption coefficient [(atm cm)$^{-1}$], q_i the average gas mixing ratio in the layer, P_e the effective pressure [atm] and l_e the effective length [cm]. The absorption coefficient is strongly dependent on pressure in the altitudes considered for this study and only weakly dependent on temperature. The effective pressure and length can be determined using the well-known Curtis-Godson approximation (e.g., Armstrong, 1968). If the temperature is known, Eqs. (2) and (3) can be solved for mixing ratio. The "instant inversion" technique provides reasonable solutions over most of the altitude range, but there is considerable smoothing of information and fine details are lost. We are using only the formulation described by Eq. (2) as a starting point to derive a relaxation equation which will be applied in an iterative fashion to solve for mixing ratio. Thus the limitations of the "instant inversion" do not directly apply in this present work.

We start with the assumption that there are two broad spectral filters each containing emission due to two primary gases and other more tenuous species. The transmittance can be represented by the product $\tau = \tau_1\tau_2\tau_0$, where τ_1 is the transmittance due to constituent 1 (e.g., NO_2), τ_2 is due to constituent 2 (e.g., H_2O), and τ_0 is due to other less absorbing contaminant gases. If we differentiate (2) with respect to gas 1 and 2 holding τ_0 constant, we have

$$dN = -B(\tau_1\tau_0 d\tau_2 + \tau_2\tau_0 d\tau_1), \qquad (4)$$

where the arguments have been dropped for simplicity. If it is assumed that the change in K_i for a given change in q_i (and hence P_e) is small, it can be shown that

$$d\tau_i \approx \tau_i \ln(\tau_i) \frac{dq_i}{q_i}. \qquad (5)$$

This leads to the following relationship when (4) and (5) are combined:

$$dN = -\frac{\tau \ln(\tau_1) N dq_1}{(1 - \tau) q_1} - \frac{\tau \ln(\tau_2) N dq_2}{(1 - \tau) q_2}. \qquad (6)$$

For sufficiently large changes in q_1 and q_2, we can

use the finite-difference form of Eq. (6), where dN becomes ΔN and dq becomes Δq. The quantity ΔN is the monochromatic difference in radiance emitted by the horizon for mixing ratios q_i and $q_i + \Delta q_i$. The quantities q_i can be regarded as the first-guess mixing ratios, and Δq_i are the amounts these guesses need to be adjusted for the next iteration. The total band difference over the range of filter 1 with spectral instrument function $\phi_1(\nu)$ is

$$\Delta N_1 \equiv \int_{\Delta\bar{\nu}} dN\phi_1(\nu)d\nu = -\frac{\Delta q_1}{q_1}\int_{\Delta\nu}\frac{\tau\ln(\tau_1)}{(1-\tau)}N_1\phi_1(\nu)d\nu - \frac{\Delta q_2}{q_2}\int_{\Delta\nu}\frac{\tau\ln(\tau_2)}{(1-\tau)}N_1\phi_1(\nu)d\nu, \quad (7)$$

where N_1 is the calculated outgoing monochromatic radiance emitted by the horizon at a wavenumber ν in filter region $\phi_1(\nu)$. A similar equation exists for filter 2. Each filter is located spectrally such that the transmittance in that filter region is dominated by one of the gases being observed. Therefore, at each tangent altitude, there exists a set of two simultaneous linear equations which can be used to solve for the corrections, Δq_1 and Δq_2, to the first guess mixing ratios at that altitude, i.e.,

$$\left.\begin{aligned}\Delta N_1 &= A_1\Delta q_1 + B_1\Delta q_2\\ \Delta N_2 &= A_2\Delta q_1 + B_2\Delta q_2\end{aligned}\right\}, \quad (8)$$

where

$$\left.\begin{aligned}A_1 &= -\int_{\Delta\bar{\nu}}\frac{\tau\ln(\tau_1)}{q_1(1-\tau)}N_1\phi_1(\nu)d\nu\\ B_1 &= -\int_{\Delta\bar{\nu}}\frac{\tau\ln(\tau_2)}{q_2(1-\tau)}N_1\phi_1(\nu)d\nu\end{aligned}\right\}. \quad (9)$$

Similar relations exist for A_2 and B_2. It is recalled that Eq. (9) is developed for monochromatic calculations. In practice, we calculate transmittance and hence radiance using the Goody (1964) band model which, in this case gives average transmittance values over five wavenumber intervals. We have computed band model coefficients for NO_2 and H_2O, but we used empirically determined values for HNO_3 and CF_2Cl_2 (Goldman *et al.*, 1971, 1976). The use of the band model greatly reduces computation time, but it also leads to inaccuracies when the integrations in (9) are carried out. This is not serious, however, since (9) is only used to update the guess for the next iteration. Results in a later section show quick and accurate convergence. In applying these relaxation equations, the τ used is for the entire horizontal path, not just the tanget layer value, but the q values incremented are the tangent layer values. This provides quicker and more stable relaxation. Several approaches can be followed from this point. The "onion-peeling" inversion can be used in which iteration occurs at each tangent altitude starting at the top layer and working downward. Each layer is iterated until radiance convergence is achieved to within the noise limit of the channel having the largest noise. The "onion-peeling" method has the advantage that the solution before and after the tangent layer can be fixed so that iteration occurs only for the tangent layer. This facilitates improved programming efficiency and potentially can reduce total computer time. On the other hand, the "onion-peeling" approach has the disadvantage that it is more subject to instability, and it tends to amplify errors. Another approach is to use Eq. (8) to correct the first guesses over the full range of altitudes. In this case the rms radiance difference determined using all levels is compared to instrument noise as a convergence criterion. This approach provides more uniform convergence behavior and is not as sensitive to errors as the "onion-peeling" inversion. A third method which will be tested soon is the nonlinear inversion developed by Mill and Drayson (1977) which, in a sense, is a reverse "onion-peeling" approach where iteration starts at the lowest altitude and works upward. This method provides the advantages of the "onion-peeling" approach and avoids many of the disadvantages. We have adopted the full-range method for the present calculations.

3. Simulation study

We have performed a study which simulated the entire experiment. Synthetic radiance profiles for NO_2, H_2O and HNO_3 were generated using data selected from among the many data sets available in the published literature (e.g., see Harries, 1976, Evans *et al.*, 1977). The CF_2Cl_2 data used were based on ground level measurements by Rasmussen (1978), assuming a constant tropospheric mixing ratio profile, and using a stratospheric shape predicted by models (Cicerone, 1977).[1] We next injected radiance errors typical of those expected from the operation of existing space systems. These included random radiance noise (0.0002–0.001 W m^{-2} sr^{-1}), radiance bias errors (0.0001–0.0005 W m^{-2} sr^{-1}), radiance scale errors of 1%, radiance errors introduced due to uncertainty in repeatability of angular spacing of radiance measurements on the limb [equivalent of 0.04 km(1σ)], and radiance errors caused by unaccounted for angular rates injected by motion of the measurement platform which would tend to stretch or compress the angular spacing of radiance measurement points (equivalent to 0.002 deg s^{-1} attitude rate error).

[1] Private communication, University of California at San Diego.

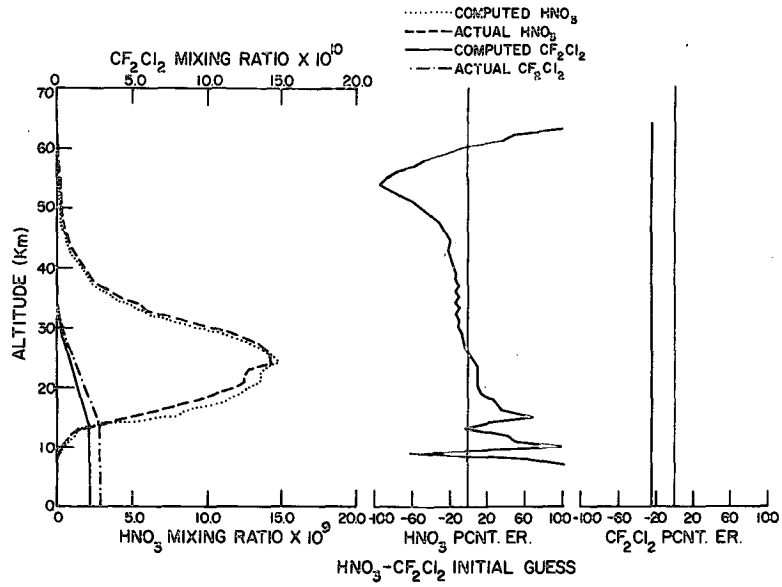

FIG. 4. Results of HNO_3 initial guess procedure.

A Gaussian-type field-of-view function $\gamma(\theta)$ was used to study the effects of spatial averaging. Deconvolution of the radiances was performed using the method of Brault and White (1971) which was first applied to limb sounding by Gille and Bailey (1978). This method is based on Fourier transform operations which lend themselves to objective data smoothing procedures. In the simulation, spatially averaged radiances were calculated by convolving $\gamma(\theta)$ with infinite resolution radiances in angle space. Noise was then added, and the Fourier transform of the radiance was performed and divided by the Fourier transform of $\gamma(\theta)$. Various apodizing methods were studied in Fourier space to provide smoothing. A method was selected that provided the greatest restoration of the infinite resolution radiance and the least noise. After apodization, the inverse transform was taken to "deconvolve" the effects of the field of view. These simulated "measured" radiance profiles were then used to test the inversion algorithms described previously. Radiance profiles with zero errors were also inverted to gain insight regarding the inversion routines. These studies allowed us to estimate expected measurement accuracies for the various gases used in the calculations.

4. Initial guess procedure

An important factor in obtaining quick convergence is a good initial guess profile that can be used to obtain the Δq_i parameters for the first iteration. In this section, we describe the first-guess methods used for each gas. The simultaneous algorithm results are presented in the final section of this paper. If absorption is small (e.g., HNO_3), the weak line approximation is valid and Eqs. (2) and (3) can be solved directly for mixing ratio by expanding the exponential function, dropping higher order transmittance terms, and integrating over the spectral band to obtain

$$q_i = N_T \left[P_e l_e \int_{\Delta\nu} B(\nu,T) K_i d\nu \right]^{-1}, \qquad (10)$$

where N_T is the radiance emitted by the tangent layer. The value of N_T is found by calculating radiance contributions for shells before and after the tangent layer and subtracting these contributions from the total observed radiance. This was done for HNO_3 by estimating radiance per path length values for higher altitude layers and then applying these values to the ray path of interest. Fig. 4 is an example of this initial guess approach for HNO_3 when the observed radiance errors are zero. The CF_2Cl_2 initial guess is obtained by taking a fixed percentage of the true profile. In practice, ground-based data and model profiles should provide a very good CF_2Cl_2 guess. When absorption is stronger such as in the NO_2 and H_2O bands, the simple relation [Eq. (10)] used for HNO_3 does not apply and a different initial guess procedure must be used. If Eq. (10) is used for NO_2 and H_2O, the mixing ratio profile shape tends to be preserved, but the magnitude is underestimated. The approach we followed was to use (10) but normalize the peak mixing ratio to a peak value for a mean stratospheric profile (12 ppb for NO_2 and 4 ppm for H_2O).

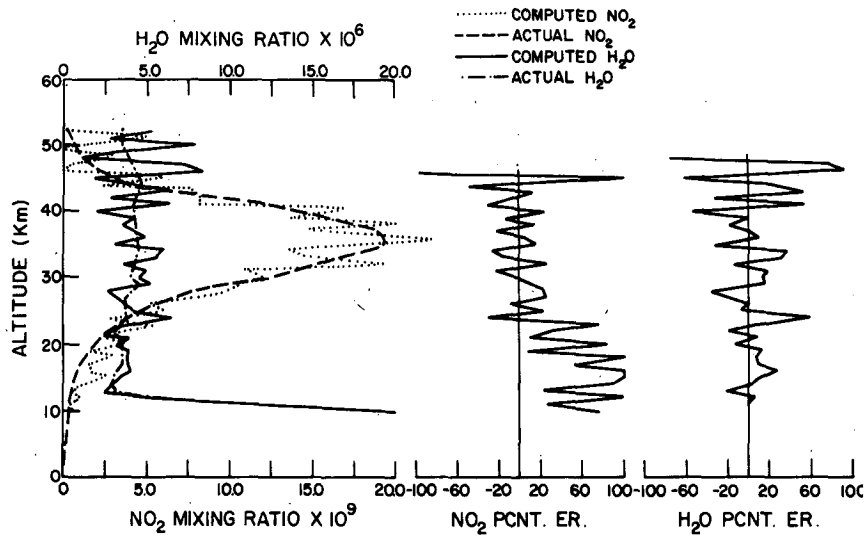

FIG. 5. Unsmoothed NO_2–H_2O inversion results for an infinitesimal spatial field of view.

5. Simultaneous inversion algorithm results

Starting with first guesses obtained by the methods just described, the simultaneous inversion algorithm was then applied to radiances for all four gases considered in this study. The spectral filter locations and shapes of Fig. 1 were used for NO_2 and H_2O. The filters used in the HNO_3–CF_2Cl_2 study were based on the LIMS HNO_3 filter and an idealized trapezoidal-shaped filter centered at 10.8 μm for CF_2Cl_2. The unsmoothed, infinitesimal field-of-view NO_2–H_2O results are shown in Fig. 5, and the smoothed spatially-averaged results with deconvolution applied are shown in Fig. 6. Note the error reduction provided by the Fourier smoothing procedure. The rms error in concentration is ~15% over the 15–45 km altitude range for both H_2O and NO_2. Also note the H_2O profile features that are preserved near the tropopause by the deconvolution procedure. Similar calculations were done for a much lower NO_2 concentration (~3 ppbv), and the simultaneous inversion gave virtually identical H_2O results but a poorer NO_2 solution. This is expected due to the lower signal-to-noise ratio (NO_2 rms errors ~50–60% from 15 to 40 km). One reason this is true is because H_2O is a dominant emitter in com-

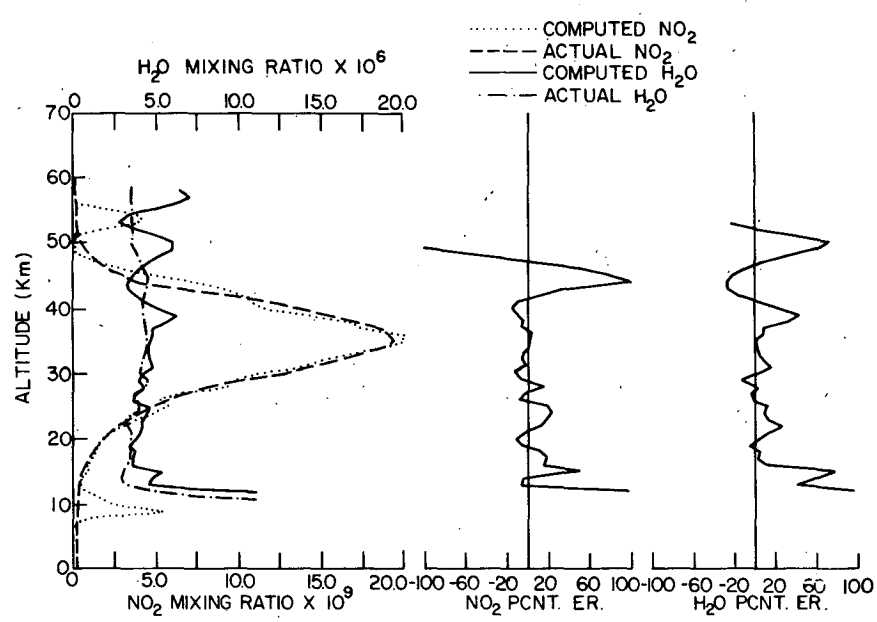

FIG. 6. Smoothed, deconvolved inversion results for noisy, spatially averaged NO_2–H_2O radiances.

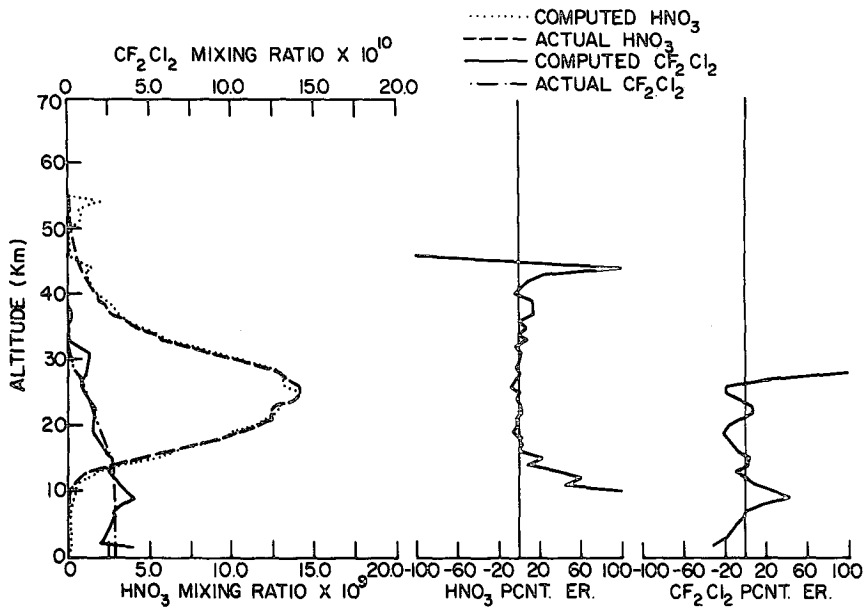

FIG. 7. Smoothed, deconvolved inversion results for noisy, spatially averaged HNO_3–CF_2Cl_2 radiances.

parison to NO_2. If the two emitters are comparable in radiance, errors are more interdependent. We simulated this situation to some extent by shifting the H_2O filter (Fig. 1) so that it totally overlapped the NO_2 band, giving a greater NO_2 contribution in the H_2O filter region. We found that results for both gases were degraded. The degradation of the H_2O results was more pronounced (rms error being nearly 50% higher for the overlapping case) due to the increased NO_2 signature in the H_2O channel. However, computing time and speed of relaxation were nearly unaffected. These results suggest that the radiance contribution of the minor emitter should be no more than ~15–20% of the total radiance in order for accurate inversions to be obtained.

The smoothed HNO_3–CF_2Cl_2 results in Fig. 7 give HNO_3 errors of <10% from 15–40 km and CF_2Cl_2 errors <20% up to 20 km. Simulations using a much lower concentration HNO_3 profile revealed similar results in both channels. These findings are encouraging and suggest that it is feasible to measure CF_2Cl_2 using the limb emission experiment. As already noted, the noise values and other errors used in the simulations were selected based on existing satellite instrumentation. Also, if several profiles are averaged together in latitude bands in a zonal direction, even better CF_2Cl_2 accuracy could be achieved. There are other factors we did not include, such as errors introduced by uncertainties in aerosol emission. We are presently estimating the magnitude of these effects.

The algorithm developed in this research behaves very smoothly. No more than three iterations, and sometimes only two, are needed for a solution. The algorithm provides the advantages of a single inversion yet gives a double inversion with only a modest increase in computer time.

Acknowledgments. We would like to acknowledge the helpful discussions and suggestions by Dr. John Gille and Mr. Paul Bailey concerning the application of Fourier deconvolution procedures to limb radiances.

REFERENCES

Armstrong, Baxter, H., 1968: Analysis of the Curtis Godsen approximation and radiation transmission through inhomogeneous atmospheres. *J. Atmos. Sci.*, 25, 312–322.

Brault, J. W., and O. R. White, 1971: The analysis and restoration of astronomical data via the fast Fourier transform. *Astron. Astrophys.*, 12, 169–189.

Evans, W. J. R., J. B. Kerr, C. T. McElroy, R. S. O'Brien, B. A. Ridley and D. J. Wardle, 1977: The old nitrogen mixing ratio in the stratosphere. *Geophys. Res. Lett.*, 4, 235–238.

Gille, John C., and F. B. House, 1971: On the inversion of limb radiance measurements I: Temperature and thickness. *J. Atmos. Sci.*, 28, 1427–1442.

——, and Paul L. Bailey, 1978: Information content and results of non-linear inversion of Nimbus 6 limb radiance inversion radiometer data. *Remote Sensing of the Atmosphere: Inversion Methods and Applications*, A. L. Fymat and V. E. Zeuev, Eds., Elsevier, 107–113.

Goldman, A., T. G. Kyle and F. S. Bonomo, 1971: Statistical band model parameters and integrated intensities for the 5.9 μm, 7.5 μm, and 11.3 μm bands of HNO_3 vapor. *Appl. Opt.*, 10, 65–73.

——, F. S. Bonomo and D. G. Murcray, 1976: Statistical band model analysis and integrated intensity for the 10.8 μm band of CF_2Cl_2. *Geophys. Res. Lett.*, 3, 309–312.

Goody, R. M., 1964: *Atmospheric Radiation I. Theoretical Basis*. Oxford University Press (see pp. 4–36).

Harries, J. E., 1976: The distribution of water vapor in the stratosphere. *Rev. Geophys. Space Phys.*, 14, 565–575.

House, F. B., and G. Ohring, 1969: Inference of stratospheric

temperature and moisture profiles from observations of the infrared horizon. NASA CR-1419.

Mill, J. D., and S. R. Drayson, 1977: A nonlinear technique for inverting limb absorption profiles. *Remote Sensing of the Atmosphere: Inversion Methods and Applications*, A. L. Fymat and V. E. Zeuev, Eds., Elsevier, 123–135.

Rasmussen, R. A., 1978: Status report on global CFM measurements. Paper presented at the WMO Symposium on the Geophysical Aspects and Consequences of Changes in the Composition of the Stratosphere, Toronto, June.

Russell, James M., III, Park, Jae H. and S. R. Drayson, 1977: Global monitoring of stratospheric halogen compounds from a satellite using gas filter spectroscopy in the solar occultation mode. *Appl. Opt.*, **16**, 607–612.